Korean J. of Chem. Eng., **4**(2) (1987) *135-142*

A NUMERICAL ANALYSIS OF RATE DATA FOR PACKED BED REACTORS IN GAS-SOLID REACTION SYSTEMS

Heung Chul PARK and Hee MOON

Dept. of Chemical Process, College of Engineering, Chonnam National University, Kwangju 500, Korea

(Received 4 October 1986 • accepted 28 February 1987)

Abstract—A numerical solution of the pseudo-steady state governing equations on the basis of the Langmuir-Hinshelwood type rate equation was obtained by the approximate finite difference method in packed bed reactors for gas-solid reaction system. It was proved that the numerical method has good accuracy compared with the strict solution in the special case that the reaction rate can be represented by the first-order kinetics in terms of gaseous reactant and the effectiveness factor is unity druing the reaction.

The numerical method is proposed to predict the transient of exit-gas compositions of a packed bed reactor used for gas-solid reaction systems. The exit-gas composition can be predicted from the conversion data of a single particle with varying reaction time. The present method can be easily applied to the systems involving adsorptive gaseous reactants and complex reaction behavior with structural changes of particles.

INTRODUCTION

A typical reactor for non-catalytic gas-solid reactions is the packed bed type [1-6]. Since the packed bed reactor is operated under unsteady state conditions, it has been known to be very difficult to obtain the optimal design basis.

To investigate the transient behavior of the reactor, an appropriate model is set up and the governing equations describing the differential material and energy balances are solved. There are problems in the application of the proposed models because they have complex solution procedures [7-10]. The reaction between gas and solid is transient because of the direct participation of solid phase. When significant structural change in the solid phase is accompanied by a reaction, the reaction behavior can not be represented by explicit functional formulas in terms of the conversion of solid. In such cases, more simplified and practical methods are presently required.

Present work deals with a simple pseudo-steady state approximation to analyze the differential governing equations [11,12] for packed bed reactors. The simplified design procedure for packed bed reactors applicable to general gas-solid reactions involving adsorptive gaseous reactants and complicated structural change of solid is proposed.

The reaction behavior in packed bed reactors is investigated by the proposed method on the basis of the Langmuir-Hinshelwood type (L-H) rate equations. The differences in the reactor behavior between the L-H kinetics and first-order kinetics are discussed in detail.

MATHEMATICAL DESCRIPTION OF PACKED BED REACTOR

Basic Equations

The conventional packed bed reactor with all of its associated symbols is shown schematically in Fig. 1, in which the following general reversible gas-solid reaction proceeds under isothermal conditions:

$$A(g)+bB(s) \rightleftharpoons pP(g)+qQ(s) \quad (1)$$

Assuming a plug flow of gas, the differential material balance with respect to each of the gas and spherical solid reactants may be represented by:

$$u_0\frac{\partial C_A}{\partial z}+\frac{3D_e(1-\varepsilon_0)}{\varepsilon_0 R}\left(\frac{\partial C_{Al}}{\partial r}\right)_{r=R}+\frac{\partial C_A}{\partial t}=0 \quad (2)$$

$$\frac{D_e}{r^2}\frac{\partial}{\partial r}\left(r^2\frac{\partial C_{Al}}{\partial r}\right)+\frac{\partial C_B}{\partial t}=0 \quad (3)$$

$$-r_A=-\frac{\partial C_A}{\partial t}=-\frac{1}{b}\frac{\partial C_B}{\partial t} \quad (4\text{-}1)$$

$$-\frac{\partial C_B}{\partial t}=bkF(C_{Al})\,G(C_B) \quad (4\text{-}2)$$

The boundary and initial conditions are:

$$C_A=C_{AO} \quad \text{at } z=0 \quad \text{for } t\geqq 0$$

$$C_{Al}=C_A \quad \text{at } r=R \quad \text{for } t\geqq 0$$

$$\partial C_{Al}/\partial r=0 \quad \text{at } r=0$$

$$C_A=0 \quad \text{at } t=0 \quad \text{for } z>0$$

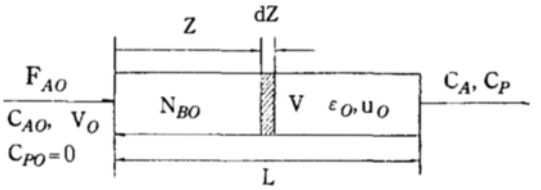

Fig. 1. Packed bed reactor with all associated symbols.

$$C_{Ai}=0 \quad \text{at } t=0 \quad \text{for } z\geqq 0,\ 0\leqq r\leqq R$$

$$C_B=C_{BO} \quad \text{at } t=0 \quad \text{for } z\geqq 0,\ 0\leqq r\leqq R$$

where C_A is the gaseous reactant concentration in the bulk stream and C_{Ai} is that in the particle.

Defining X_B as the overall conversion of particles at location z, that is, $X_B=1-\bar{C}_B/C_{BO}$, the consumption rate of the gaseous reactant at location z is represented by:

$$\frac{3D_e(1-\varepsilon_0)}{R}\left(\frac{\partial C_{Ai}}{\partial r}\right)_{r=R}=(1-\varepsilon_0)\,C_{Bo}\frac{\partial X_B}{\partial t} \tag{5}$$

The effective factor is defined by [13]:

$$\eta=\frac{\text{acutual reaction rate}}{\text{reaction rate obtainable under the conditions of the bulk gas stream,}}$$

and the over all conversion rate at location z is given as:

$$\frac{\partial X_B}{\partial t}=bkF(C_A)\ \eta\ (1-X_B) \tag{6}$$

Then, Eqs. (2)-(4) may be transformed into dimensionless formulae as shown,

$$\frac{\partial y}{\partial \lambda}+\frac{\partial X_B}{\partial \bar{\theta}}+\alpha\frac{\partial y}{\partial \bar{\theta}}=0 \tag{7}$$

$$\frac{\partial X_B}{\partial \bar{\theta}}=K_r f(y)\ g(X_B) \tag{8}$$

where $y=C_A/C_{AO}$, $\lambda=Z/L$, $\bar{\theta}=t/\tau$, $K_r=b\,k\,C_{AO}\,\tau$, $\alpha=V\varepsilon_o/v_o\tau$, and τ is the time factor defined by:

$$\tau=\frac{C_{BO}(1-\varepsilon_0)V}{b\,v_0\,C_{AO}}=\frac{N_{BO}}{bF_{AO}} \tag{9}$$

In Eq. (8), $g(X_B)$ signifies the dependency of over-all conversion rate on solid reactant and is defined by:

$$g(X_B)=\eta\ (1-X_B) \tag{10}$$

The effectiveness factor η should be given by the solution of Eqs. (3) and (4) with the relevant boundary and initial conditions.

From a practical point of view, the value of α is very small in the range of 10^{-3} to 10^{-5} for gas-solid reactions. In this case, the pseudo-steady state approximation becomes a good assumption to simplify the governing equations for a packed bed reactor as:

$$\frac{\partial y}{\partial \lambda}+\frac{\partial X_B}{\partial \bar{\theta}}=0 \tag{11}$$

Then, the corresponding initial and boundary conditions become:

$$y=1 \quad \text{at } \lambda=0 \quad \text{for } \bar{\theta}\geqq 0 \tag{12}$$

$$X_B=0 \quad \text{at } \bar{\theta}=0 \quad \text{for } \lambda\geqq 0 \tag{13}$$

In usual situations, $g(X_B)$ can not be represented by a simple function with respect to the conversion of solid reactants since the effectiveness factor η varies with reaction time in the non-catalytic gas-solid reactions in contrast to the catalytic gas-solid reactions [14-17]. Thus, Eq. (8) usually becomes a nonlinear differential equation and a numerical technique in needed to obtain solutions of Eqs. (8) and (11).

Numerical Solutions

In order to obtain the numerical solutions, the packed bed reactor is divided into N sections of equal length. The network of grid points is outlined in Fig. 2. The vertical line at the left hand side ($\lambda=0$) represents the boundary conditions at the bed inlet and the first horizontal line ($\bar{\theta}=0$) represents the initial condition. In this case, the explicit finite difference method is suitable. Then, Eqs. (8) and (11) can be written as follows:

$$y_i=y_{i-1}-\Delta\lambda\ K_r f(\bar{y}_i)\ g(\bar{X}_{Bi});\ i=1, 2, \cdots N \tag{14}$$

where $\bar{y}_i$ and $\bar{X}_{Bi}$ is the average value between n and n-1 steps as follows:

$$\bar{y}_i=\frac{y_{i,n-1}+y_{i,n}}{2};\ n=1, 2, \cdots \tag{15}$$

$$\bar{X}_{Bi}=\frac{X_{Bi,n-1}+X_{Bi,n}}{2};\ n=1, 2, \cdots \tag{16}$$

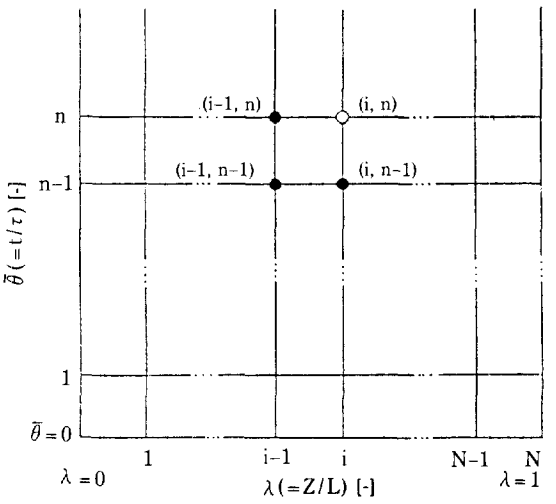

Fig 2. Network of grid points for the finite difference equation.
(●; Calculated value, ○; To be calculated value.)

The solution of Eq. (11) can be explicitly obtained by an iteration procedure to calculate the average values defined in Eqs. (15) and (16).

X_{Bi} may be obtained by the integral form of Eq. (8):

$$\int_0^{X_{Bi}} \frac{dX_B}{g(X_B)} = K_\tau \int_0^{\bar{\theta}} f(y_i)\, d\bar{\theta} \tag{17}$$

To simplify the procedure for the numerical calculation, the following approximation is employed instead of Eq. (15):

$$\bar{y}_i \simeq \bar{y}_{i-1} = \frac{y_{i-1,\,n-1} + y_{i-1,\,n}}{2} \tag{18}$$

Then, Eq. (14) reduces to:

$$y_i = y_{i-1} - \Delta\lambda\ K_\tau\ f(\bar{y}_{i-1})\ g(\bar{X}_{Bi}) \tag{19}$$

Eq. (17) becomes:

$$\int_0^{X_{Bi}} \frac{dX_B}{g(X_B)} = K_\tau \int_0^{\bar{\theta}} f(y_{i-1})\, d\bar{\theta} \tag{20}$$

Eq. (20) shows the extent of solid conversion, X_{Bi}, at the (i)th section at any time $\bar{\theta}$ is determined as a point at which the integral on the left hand side becomes equal to the known value of the integral on the right hand side evaluated for the (i-1)th section. Once X_{Bi} is known, the concentration of gas from the (i)th section at any corresponding time may be predicted by Eq. (19).

The Accuracy of the Numerical Solutions

The numerical solution of Eqs. (8) and (11) is obtained by the finite difference method using equations (19) and (20). This numerical solution can be compared with the strict solution in the special case that the reaction rate can be represented by the first order kinetics in terms of gaseous reactant and the effectiveness factor of unity during the reaction in order to determine the accuracy of the numerical method. Then, Eq. (8) becomes:

$$\frac{\partial X_B}{\partial \bar{\theta}} = K_\tau\, y\,(1 - X_B) \tag{21}$$

The strict solution of Eqs. (11) and (21) is obtained as:

$$y = \frac{e^{K_\tau(\bar{\theta}-\lambda)}}{1 - e^{-K_\tau\lambda}(1 - e^{K_\tau\bar{\theta}})} \tag{22}$$

$$X_B = 1 - \frac{1}{1 - e^{-K_\tau\lambda}(1 - e^{K_\tau\bar{\theta}})} \tag{23}$$

The concentration profile of gaseous and solid reactants in a packed bed can be calculated from Eq. (22) and (23) with respect to the dimensionless rate constant K_τ (Eq. 8) and dimensionless time $\bar{\theta}$.

On the other hand, the approximate numerical solution starts with constructing a convenient chart (Fig. 3). For this particular case, Eq. (20) reduces to

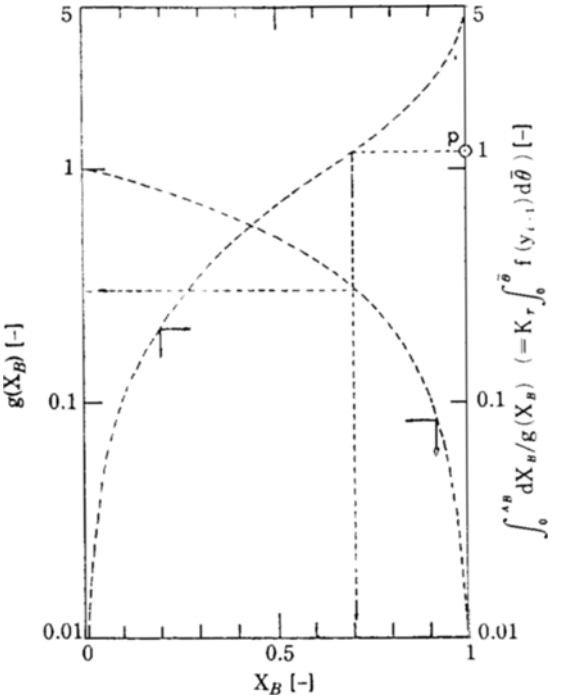

Fig. 3. Chart to be used in numerical solution, calculated for $\eta = 1$ and $f(y) = y$.

$$\ln\frac{1}{1 - X_B} = K_\tau \int_0^{\bar{\theta}} y_{i-1}\, d\bar{\theta} \tag{24}$$

Figure 3 illustrates the variation of X_B with $g(X_B)$ and the integral of $1/g(X_B)$ using $g(X_B) = 1 - X_B$.

Starting from the inlet of the reactor, where $i = 1$ and $y_0 = 1$, one can calculate the right hand side of Eq. (20) at any time, which yields $K_\tau\bar{\theta}$ by Eq. (24). The value of $K_\tau\bar{\theta}$ at any $\bar{\theta}$ is then located on the ordinate on the right hand side of Fig. 3, as shown by a point P. X_B and $g(X_B)$ at $i = 1$ at each time $\bar{\theta}$ can be evaluated from the abscissa and the ordinate on the left hand side, respectively, corresponding to the point P, as illustrated by dotted lines in the figure. The value of $g(X_B)$ at $\bar{\theta}$ allows one to evaluate y_1, at the time $\bar{\theta}$ from Eq. (19).

The integrated value of the right hand side of Eq. (20), which reduces to Eq. (24) in this case using y_1, at each time $\bar{\theta}$ should again be located on the right hand side ordinate of Fig. 3. These procedures are repeated to evaluate y_i at any time $\bar{\theta}$ at any section.

The calculated results with $N = 100$ and $\Delta\bar{\theta} = 0.002$ are shown by dashed lines in Fig. 4. As can be seen that there are no appreciable differences between the

two solutions over a wide range of K_r : However, there are small differences at the initial period.

The differences can be reduced by decreasing the time interval, $\Delta\bar{\theta}$, and by increasing the number of axial divisions N in the numerical calculation. By comparing the numerical and the strict solutions with respect to the various time intervals and the number of axial divisions, it is concluded that the numerical solutions with N=100 and $\Delta\bar{\theta}=0.002$ have fairly good accuracy compared to the strict solutions.

EFFECT OF ADSORPTIVE SPECIES IN PACKED BED REACTORS

Transient Response of Gaseous Reactant

When an adsorptive gaseous species reacts with solid, the effect of gaseous reactant on the reaction rate may often be represented by [5]:

$$f(y)=\frac{y}{1+Ky} \tag{25}$$

The solution of Eq. (25) can be obtained by numerical methods using Eqs. (19) and (20) according to the procedures described in the preceding section. The calculated break-through curves for gaseous reactant at the exit of the packed bed are shown in Fig. 5.

In order to ascertain the effect of the adsorptive species on the transient of the packed bed, the break-through curves (Fig. 5) were obtained by varying the value of K with K_r of 5 which is a typical value for the steam-iron reaction. The values of K in terms of denominator in Eqs. (8) and (25) mean that the reaction rate is restricted if the gaseous reactant is a strongly adsorptive species. Figure 5 shows accordingly that the break-through curves for gaseous reactant at the exit of a packed bed become flatter than those without the effect of adsorption, K=0.

From Figs. 4 and 5, the effect of K is the counterpart of K_r on the break-through curves since the reaction rate decreases as the effect of adsorptive species on the reaction rate increases.

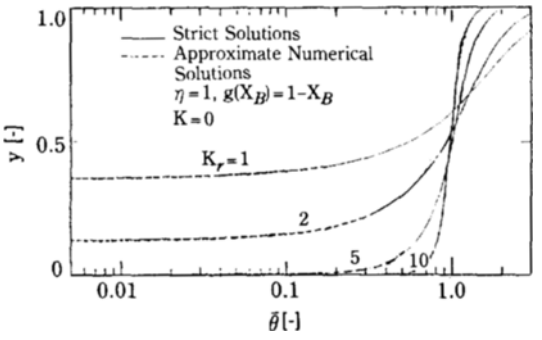

Fig. 4. Comparison between approximate numerical and strict solution for transient of gaseous reactant at exit of packed bed.

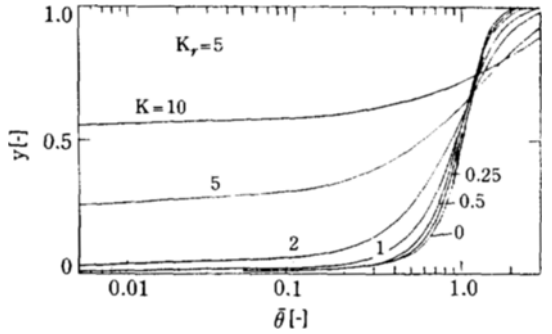

Fig. 5. Effect of k on the transient of a gaseous reactant at the exit of a bed (K_r=5).

Concentration Profiles of Solid Reactant

The concentration profiles of gaseous and solid reactant can give a precise effect of adsorptive species on the characteristics of the reaction in a packed bed reactor. Typically, solid conversions in a packed bed reactor at $\bar{\theta}=0.5$ are shown in Fig. 6 with respect to the value of K when K_r=5.

The profile of solid conversion becomes flat as K increases since the effect of adsorptive species on the reaction rate increases.

On the other hand, this is caused by the flat profile of the gases reactant conversion because of the restriction on the reaction rate.

When K>5, the reaction occurs uniformly in the all positions in the packed bed. Thus, the packed bed reactor has the similar characteristics to the differential

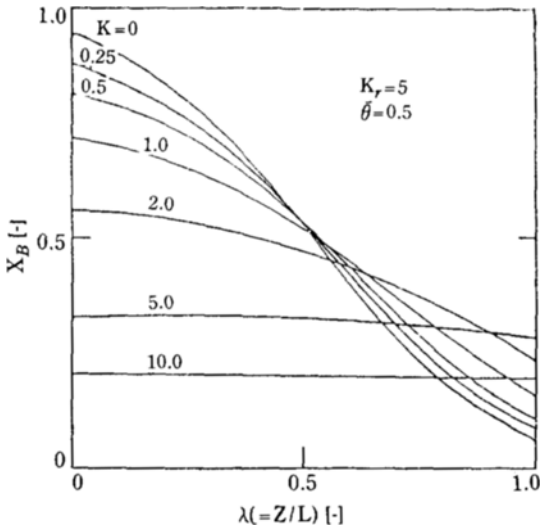

Fig. 6. Conversion profiles of solid reactant in packed bed at $\bar{\theta}$=0.5 with K_r=5.

reactors. More practical application of this phenomenon has been discussed in the previous work [19-21].

EXTENSION TO GENERAL CASE

It is well known that solid structural properties such as pore volume, pore size and pore surface area play an important role in the reaction between gas and a solid [22-28] and it progressively changes as the reaction progresses [29-36].

Systems having variation of structural properties have complex reaction behavior. Therefore, the modeling of the kinetics to represent $g(X_B)$ in Eq. (20) by an explicit functional formula in terms of X_B and the solution of the model equation become extremely complex with a little practical use. Thus, this work proposes to evaluate the dependency of the solid concentration, $g(X_B)$, on the reaction rate directly by using the rate data for single particles which obtained under the same reaction conditions as in the packed bed reactor.

The extent of conversion of solid reactant of a single particle at any time can be easily determined from a differential flow reactor. The rate of conversion, $(dX_B/dt)_{obs}$ may then be obtained by graphical differentiation of the relation between the extent of conversion and the reaction time. When the conversion rate data for a single particle are obtained under the same operating conditions as of a packed bed reactor, the dependency of reaction rate on the solid concentration, $g(X_B)$, is expressed by Eqs. (6) and (10), in general, as:

$$g(X_B) = \eta\,(1-X_B) = \frac{1}{bkF(C_A)}\left(\frac{dX_B}{dt}\right)_{obs} \qquad (26)$$

The rate data thus obtained usually contain the effects such as diffusion in the particle, adsorptive gaseous species and variation of pore structure. Therefore, the value of $g(X_B)$ obtained here directly reflects the reaction behavior of the single particles which are usually used in the reactor.

Separable Cases

When the reaction is frist-order with respect to gaseous reactant or, it is controlled by chemical reaction or diffusion, the effect of gaseous reactant concentration is not included in $g(X_B)$[37]. Thus, $g(X_B)$ is separated from the effect of gaseous reactant. In such cases, a series of data of $g(X_B)$ obtained at any concentration of gaseous reactant can be used for the calculation of the exit-gas compositions for a packed bed reactor. Then, the procedures to solve Eqs. (19) and (20) can be utilized according to the manner of the numerical solution.

Figure 7 shows $g(X_B)$ calculated from the rate data

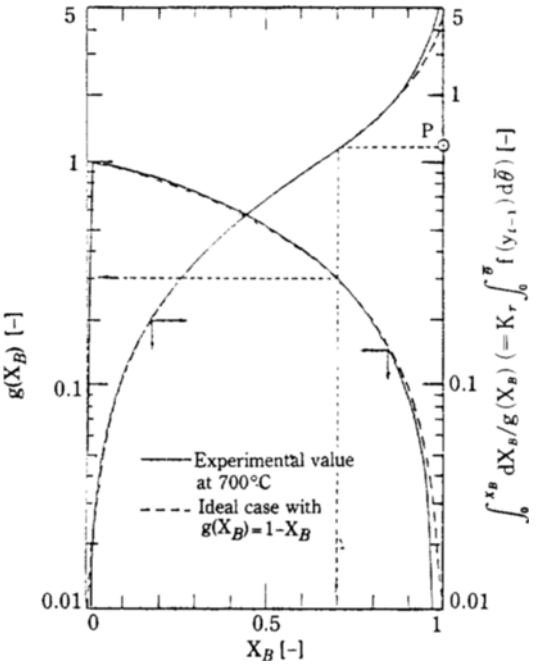

Fig. 7. Comparison of experimental data with numerical solution of ideal case.

of oxidation of porous reduced iron oxide at 700°C depicted from the previous work [20].

The experimental values of $g(X_B)$ at 700°C agree well with those of ideal case except for the begining and final stages of reaction. The lower values of $g(X_B)$ at the start of reaction is caused by the induction period existing during the begining stage [35]. The uniform oxidation of porous reduced iron oxide at 700°C also agrees with the results at high temperatures above 700°C of Turkdogan et al [25, 26]. The decrease in $g(X_B)$ at the end of reaction is considered to be the result of the slow rate of oxidation from magnetite to hematite.

Non-Separable Cases

The effectiveness factor η for a single particle system involving adsorptive gaseous reactant is influenced by the magnitude of $K = K_A C_{AO}$. Hence, $g(X_B) = \eta(1-X_B)$ is not separated from the effect of gaseous reactant in such systems.

In the packed bed reactor, the gaseous reactant concentration C_A changes along with the longitudinal location in the bed from C_{AO} at the inlet to as low as 0 at the exit. Therefore, $g(X_B)$ is needed to be evaluated on the different basis accordingly with the variation of gaseous reactant concentration. In such cases, the experiment in the differential flow reactor should be repeated at different gaseous reactant concentrations.

For each run, $g(X_B)$ is evaluated and depicted on $g(X_B)$-X_B chart. The chart can be used as follows:

Calculation starts at the inlet of the reactor, $i=1$, where Eqs. (19) and (20) reduce to:

$$y_1 = 1 - \Delta\lambda \; K_r f(1) \; g(\bar{X}_{B1}) \tag{27}$$

$$\int_0^{X_{B1}} \frac{dX_B}{g(X_B)} = K_r f(1) \; \bar{\theta} \tag{28}$$

(1) Choose the series of $g(X_B)$ evaluated at $C_A = C_{AO}$ or estimate $g(X_B)$ from those evaluated at C_A to C_{AO}.
(2) Calculate the integral on the left hand side of Eq. (28) using $g(X_B)$ obtained at the step (1).
(3) Construct the chart such as shown in Fig. 3. Then the procedures to evaluate y_1 are the same as those described previously, since the right hand side of Eq. (28) can be evaluated at any time $\bar{\theta}$.

For $i \geqq 2$, the procedures become different from those for separable case. For $i=2$, Eqs. (19) and (20) become:

$$y_2 = y_1 - \Delta\lambda \; K_r f(\bar{y}_1) \; g(\bar{X}_{B2}) \tag{29}$$

$$\int_0^{X_{B2}} \frac{dX_B}{g(X_B)} = K_r \int_0^{\bar{\theta}} f(y_1) \; d\bar{\theta} \tag{30}$$

(4) First evaluate the integral on the right hand side of Eq. (20) between $\bar{\theta}=0$ and $\Delta\bar{\theta}$, using y_1 at $\theta=0$ and $\Delta\theta$.
(5) Calculate the mean of y_1 in $=0 \sim \Delta\theta$ from Eq. (18).
(6) Assume the solid particle at $i=2$ contacts with the gas of concentration at this mean $\bar{y}_1$ during $\theta=0\sim\Delta\theta$ and estimate $g(X_B)$ at $C_A = C_{AO}\,y_1$ on the $g(X_B)$-X_B chart experimentally obtained.
(7) Evaluate the integral on the left hand side of Eq. (30) and find X_{B2} using the point at which the left hand side becomes equal to the right hand side in Eq. (30). This value is the extent of conversion of solid at $i=2$ at $\theta=\Delta\theta$, $X_{B2,1}$.
(8) Calculate y_2 at $\theta=\Delta\theta$ from Eq. (29) using $g(X_B)$ at $\bar{X}_{B2}$ in the period $\theta=0\sim\Delta\theta$.
(9) Extend the integral on the right hand side of Eq. (30) to $\theta=0\sim2\Delta\theta$.
(10) Calculate the mean of y_1 in the period of $\theta=\Delta\theta\sim2\Delta\theta$.
(11) Estimate $g(X_B)$ at $C_A = C_{AO}\,\bar{y}_1$, which is the mean during $\theta=\Delta\theta\sim2\Delta\theta$, in the $g(X_B)$-X_B chart.
(12) Evaluate the integral on the left hand side of Eq. (30). Use $g(X_B)$ obtained from the step (6) for $X_B = 0 \sim X_{B2,1}$ and $g(X_B)$ from the step (11) for $X_{B2} > X_{B2,1}$. Find $X_{B2,2}$ at $\theta=2\Delta\theta$ as a extent where the equivalence of Eq. (30) holds.
(13) Calculate y_2 at $\theta=2\Delta\theta$ from Eq. (29) using $g(X_B)$ at $X_{B2,2}$ in $\theta=\Delta\theta\sim2\Delta\theta$.

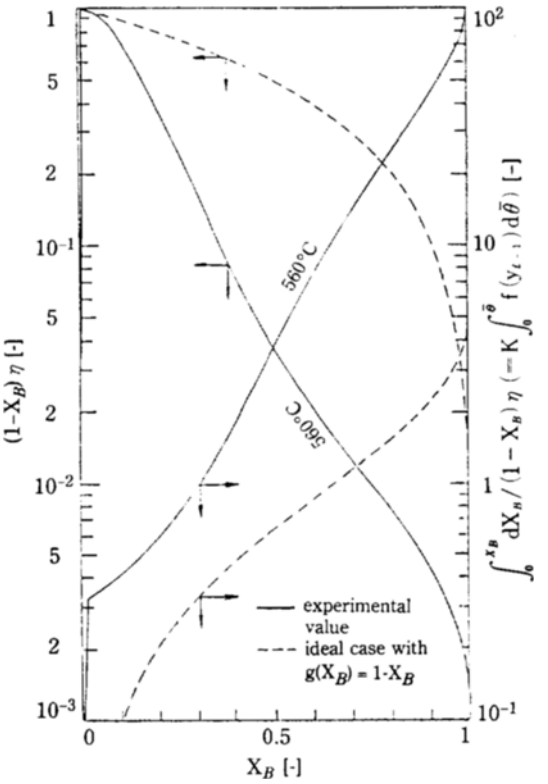

Fig. 8. Deviation between experimental data and numerical results for an ideal case with $g(X_B)=1-X_B$.

(14) The same procedures are repeated to evaluate X_{B2} and y_2 at $\theta=3\Delta\theta$, $4\Delta\theta$, -----.

The procedures for $i \geqq 3$ are the same as those described above for $i=2$.

Figure 8 illustrates $g(X_B)$ calculated from the rate data of oxidation of porous reduced iron oxide at 560°C depicted from the previous work [20] for use of non-separable cases. The figure also shows an ideal case of $g(X_B)=1-X_B$ for comparison with the actual results. The integral of $1/g(X_B)$ with respect to X_B can be calculated by using these data of $g(X_B)$. The value of $g(X_B)$ for this temperature is significantly different from that of uniform conversion. This is considered to be caused by the structural changes of solid phases [20], i. e. Path I, $Fe \rightarrow Fe_3O_4 \rightarrow Fe_2O_3$ below 570°C and Path II, $Fe \rightarrow FeO \rightarrow Fe_3O_4 \rightarrow Fe_2O_3$ above 570°C. The observed conversions were explained in terms of structural changes at different temperatures as above. To clarify this point, however, one needs more information about the solid structure, which is not dealt with in this paper. The results are shown in Fig. 8. which can be

used for numerical solution of the transient analysis of exit-gas composition in packed beds [19].

CONCLUSIONS

The numerical solution of the pseudo-steady state governing equations on the basis of the Langmuir-Hinshelwood type rate equation was obtained by the approximate finite difference method. It was proved that the numerical method has good accuracy compared with the strict solution in the special case that the reaction rate can be represented by first-order kinetics in terms of gaseous reactant and the effectiveness factor is unity during the reaction.

The rate equation of the L-H types with the adsorptive effect of gaseous reactant should be used in the transient analysis of exit-gas compositions for the packed bed reactor which involves strongly adsorptive gaseous reactants on solid reactant.

The extension of analysis of packed bed reactors to practical situations, including those where structural change greatly affects the reaction rate, is made possible by introducing a simple approach for evaluating the dependency of solid reactant on the reaction rate, $g(X_B)$, from single particle rate data obtained in differential flow reactors.

ACKNOWLEDGEMENT

The authors gratefully acknowledge the financial support of Korea Science and Engineering Foundation for this work.

NOMENCLATURE

- A : gaseous reactant in Eq. (1) [-]
- B : solid reactant in Eq. (1) [-]
- b : stoichiometric coefficient in Eq. (1) [-]
- C_A : gaseous reactant concentration [mol/m^3]
- C_{AO} : gaseous reactant concentration in feed stream [mol/m^3]
- C_B : solid reactant concentration [mol/m^3]
- C_{BO} : solid reactant concentration at initial state [mol/m^3]
- C_P : concentration of gaseous product [mol/m^3]
- C_{PO} : concentration of gaseous product at the inlet of the reactor [mol/m^3]
- D_e : effective diffusivity [m^2/min]
- $F(C_A)$: dependency of conversion rate on gaseous reactant concentration [mol/m^3]
- F_{AO} : molar feed rate of gaseous reactant [mol/min]
- f(y) : defined by Eq. (25) [-]
- $f(C_A)$: dimensionless form of $F(C_A)/C_{AO}$ [-]
- $G(C_B)$: dependency of conversion rate on solid reactant concentration [mol/m^3]
- $g(X_B)$: defined by Eq. (10) [-]
- K : a constant defined by $K = K_A C_{AO}$ [-]
- K_A : adsorption equilibrium constant [m^3/mol]
- K_r : a constant defined by $K_r = b\ k\ C_{AO}\ \tau$ [-]
- k : rate constant [m^3/mol·min]
- L : bed length of the reactor [m]
- N : number of sections of equally divided bed [-]
- N_{BO} : moles of solid reactant packed in the bed [mol]
- P : gaseous product in Eq. (1) [-]
- p : stoichiometric coefficient in Eq. (1) [-]
- Q : solid product in Eq. (1) [-]
- q : stoichiometric coefficient in Eq. (1) [-]
- R : diameter of sample particles [m]
- r : radial position from center of particle [m]
- $-r_A$: reaction rate based on unit volume of reacting solid [mol/m^3·min]
- t : reaction time [min]
- u_0 : $v_0\ L/V\ \varepsilon_0$, gas velocity in the bed [m/min]
- V : bed volume of reactor [m^3]
- v_0 : volumetric flow rate of reactant gas [m^3/min]
- X_B : overall conversion of solid reactant [-]
- $(dX_B/dt)_{obs}$: observed reaction rate [1/min]
- y : C_A/C_{AO}, unconverted fraction of gaseous reactant [-]
- Z : length of the packed bed [m]

Greek Letters

- α : accumulation factor [-]
- η : effectiveness factor for gas-solid reaction [-]
- ε_0 : void fraction of the bed [-]
- θ : t/τ, dimensionless reaction time [-]
- $\Delta\lambda$: λ/N [-]
- λ : Z/L [-]
- τ : $N_{BO}/b\ F_{AO} = C_{BO}\ (1-\varepsilon_0)V/b\ v_0\ C_{AO}$, time factor [min].

Subscripts

- (g) : gas
- (s) : solid
- m : mean value
- i : in the particle, value of the (i)th section
- n : value of the (n)th section

Superscript

- – : mean value

REFERENCES

1. Landeghem, H.V.: *Chem. Eng. Sci.*, **35**, 1912 (1980).

2. Levenspiel, O.: Chemical Reactipn Engineering, 2nd ed., John wiley, New York, 1972.
3. Lyczkowski, R.W.: *Can. J. of Chem. Eng.*, **60,** 61 (1982).
4. Shah, Y.T.: Gas-Liquid-Solid Reactor Design, McGraw-Hill, New York, 1979.
5. Szekely, J., Evans, J.W. and Sohn, H.Y.: Gas-Solid Reactions, Academic Press, New York, 1976.
6. Thones, O.: *Chem. Eng. Sci.*, **35,** 1840 (1980).
7. Fan, L.S., Miyanami, K. and Fan, L.T.: *Chem. Eng. J.*, **13,** 13 (1977).
8. Farrior, Jr., W.L., Poston, Jr., A.M. and Oldaker, E.C.: Regenerable Iron Oxide-Silica Sorbents for the Removal of H_2S from Hot Producer Gas, Preprint for the 4-th Energy Resources Conference, Lexington, Kentucky, 1976.
9. Shettigar, U.R. and Hughes, R.: *Chem. Eng. J.*, **3,** 93 (1972).
10. Wen, C.Y.: *Ind. Eng. Chem.*, **60**(9), 34 (1968).
11. Bischoff, K.B.: *Chem. Eng. Sci.*, **20,** 783 (1965).
12. Bowen, J.R.: *Chem. Eng. Sci.*, **20,** 712 (1965).
13. Ishida, M. and Wen, C.Y.: *Chem. Eng. Sci.*, **23,** 125 (1968).
14. Bischoff, K.B.: *Chem. Eng. Sci.*, **22,** 525 (1967).
15. Satterfield, C.N.: Mass Transfer in Heterogenous Catalysis, M.I.T. Press, Massachusetts, 1970.
16. Thiele, E.W.: *Ind. Eng. Chem.*, **31,** 916 (1939).
17. Weisz, P.B. and Hicks, J.S.: *Chem. Eng. Sci.*, **17,** 265 (1962).
18. Rosenberg, D.U.: Methods for the Numerical Solution of Partial Differential Equation, Elservier Pub., 1969.
19. Park, H.C., Kimura, S., Sakai, Y., Tone, S. and Otake, T.: *J. of Chem. Eng. Japan*, **17**(3), 269 (1984).
20. Park, H.C., Kimura, S., Sakai, Y., Tone, S. and Otake, T.: *J. of Chem. Eng. Japan*, **17**(4), 395 (1984).
21. Park, H.C. and Moon, H.: *Korean J. Chem. Eng.*, **1**(2), 165 (1984).
22. Krasuk, J.H. and Smith, J.M.: *AIChE J.* **18,** 506 (1972).
23. Sampath, B.S. and Hughes, R.: *Chem. Engr. (London)*, **278,** 485 (1973).
24. Turkdogan, E.T. and Vinters, J.V.: *Met. Trans.*,**2,** 3175 (1971).
25. Turkdogan, E.T., Olsson, R.G. and Vinters, J.V.: *Met. Trans.*, **2,** 3189 (1971).
26. Turkdogan, E.T. and Vinters, J.V.: *Met. Trans.*, **3,** 1561 (1972).
27. Weisz, P.B. and Goodwin, R.D.: *J. Catalysis*, **2,** 397 (1963).
28. Weisz, P.B. and Goodwin, R.D.: *J. Catalysis*, **6,** 227 (1966).
29. Bhatia, S.K. and Perlmutter, D.D.: *AIChE J.*, **27,** 226 (1981).
30. Bhatia, S.K. and Perlmutter, D.D.: *AIChE J.*, **27,** 247 (1981).
31. Deb Roy, T. and Abraham, K.P.: *Met. Trans.*, **5,** 349 (1974).
32. Dogu, T.: *Chem. Eng. Sci.*: **36,** 213 (1981).
33. Dutta, S., Wen, C.Y. and Belt, R.J.: *Ind. Eng. Chem., Process Des. Dev.*, **16,** 20 (1977).
34. King, R.P. and Brown, C.P.: *Met. Trans.*, **11B,** 585 (1980).
35. Rao, Y.K.: *Met. Trans.*, **10B,** 243 (1979).
36. Sohn, H.Y. and Sohn, H.J.: *Ind. Eng. Chem., Process Des. Dev.*, **19,** 237 (1980).
37. Kimura, S., Nakagawa, J., Tone, S. and Otake, T.: *J. of Chem. Eng. Japan*, **14,** 190 (1981).